Electrodeposited Ni–Fe–C Cathodes for Hydrogen Evolution

Shinsaku Meguro, Teruhito Sasaki, Hiroshi Katagiri, Hiroki Habazaki, Asahi Kawashima, Takashi Sakaki, Katsuhiko Asami and Koji Hashimoto

J. Electrochem. Soc. 2000, Volume 147, Issue 8, Pages 3003-3009.
doi: 10.1149/1.1393639

Journal of The Electrochemical Society, **147** (8) 3003-3009 (2000)
S0013-4651(00)01-083-1 CCC: $7.00 © The Electrochemical Society, Inc.

Electrodeposited Ni-Fe-C Cathodes for Hydrogen Evolution

Shinsaku Meguro,[a] Teruhito Sasaki,[a] Hiroshi Katagiri,[a] Hiroki Habazaki,[b,*,d] Asahi Kawashima,[b,*] Takashi Sakaki,[c] Katsuhiko Asami,[b,*] and Koji Hashimoto[a,,z]**

[a]*Tohoku Institute of Technology, Sendai 982-8588, Japan*
[b]*Institute for Materials Research, Tohoku University, Sendai 980-8577, Japan*
[c]*Nanyo Research Laboratories, Tosoh Company, Shin-Nanyo 746-8501, Japan*

Tailoring of active nickel alloy cathodes for hydrogen evolution in a hot concentrated hydroxide solution was attempted by electrodeposition. Electrodeposited iron is naturally more active for hydrogen evolution than nickel, but Ni-Fe alloys show further high activity for hydrogen evolution, although the rate-determining step being assumed as proton discharge is not changed. The carbon addition to iron or nickel remarkably enhances the activity for hydrogen evolution and changes the mechanism of hydrogen evolution. Ternary Ni-Fe-C alloys show the highest activity for hydrogen evolution, and the Tafel slope of hydrogen evolution is about 33 mV/dec, suggesting the rate-determining step of desorption of adsorbed hydrogen by recombination. XPS analysis reveals that the charge transfer occurs from nickel to iron in alloys and the carbon addition particularly enhances the charge transfer. Accelerated proton discharge due to enhanced charge transfer from nickel to iron seems responsible for the high activity of the Ni-Fe-C alloys for hydrogen evolution.

Manuscript submitted January 20, 2000; revised manuscript received May 19, 2000. This was Paper 875 presented at the Honolulu, Hawaii, Meeting of the Society, October 17-22, 1999.

Enhancement of cathodic activity of nickel for electrolytic hydrogen evolution has been carried out by the formation of nickel alloys such as Ni-S,[1] Raney Ni,[2] Ni-Mo,[3-8] Raney Ri-RuO_2,[9] Ni-Sn,[10] and Ni-Mo-O.[11,12] Recently, it has been found that Ni-Mo-O cathodes prepared by arc ion plating have excellent catalytic activity and durability for hydrogen evolution in the electrolysis of hot concentrated NaOH solutions.[12] Detailed examination by some of the present authors in comparing Ni-Mo and Ni-Mo-O alloys for hydrogen evolution revealed that the high activity is attributable to the enhancement of the rate-determining electrochemical desorption of adsorbed hydrogen due to the modification of the electronic state of electrode metals by interaction with oxygen contained in the form of solid solution.[12]

In this manner, the catalytic activity for hydrogen evolution can be enhanced by modification of the electronic state of electrode metals by alloying. Since electrodeposited various electrodes such as Ni-Mo and Ni-S have considerably high activity for hydrogen evolution, electrodeposition of nickel alloys will be a potential method for production of effective cathode materials.

In the present work, active Ni-Fe-C cathodes were prepared by electrodeposition and their activity for hydrogen evolution was examined in a hot alkaline solution.

Experimental

The basic electrolyte used for electrodeposition at room temperature was an aqueous solution consisting of 1.14 M $NiSO_4 \cdot 7H_2O$, 0.19 M $NiCl_2 \cdot 6H_2O$, and 0.49 M H_3BO_3 to which 0-0.18 M $FeSO_4 \cdot 7H_2O$ and 0-0.11 M lysine were added. For preparation of Fe-C alloys electrodeposition was carried out in solutions consisting of 0.889 M$(NH_4)_2SO_4FeSO_4$ and 0.0011-0.11 M lysine. The substrates were nickel plates chemically etched in the 1:1 mixture of concentrated H_2SO_4 and HNO_3 for 30 s. Electrodeposition was carried out at 30°C and 50 A m^{-2}.

The composition of metallic elements in the electrodes thus prepared was analyzed by electron probe microanalysis, and carbon was chemically analyzed by combustion infrared absorption. The structure of the electrodes was identified by X-ray diffraction (XRD) using Cu Kα radiation. The grain size of the deposits was estimated from the full width at half maximum (fwhm) of the most intense diffraction line by Scherrer's equations.[13] X-ray photoelectron spectroscopy (XPS) was used for characterization of the surface of the electrodes. A Shimadzu ESCA 85 photoelectron spectrometer was used with Mg Kα excitation for measurements of X-ray photoelectron spectra.

The hydrogen evolution activity of the electrodes was examined in 8 M NaOH solution at 90°C. A cell of acrylic resin with the electrodes, a platinum counter electrode, and an external Hg/HgO/1 M NaOH reference electrode having a reversible potential of 0.950 V for the hydrogen reaction were used. The galvanostatic polarization curves were measured. The ohmic drop was corrected using a current interruption method.

Results

Figure 1 shows the effect of iron addition into electrodeposited nickel on the activity for hydrogen evolution in a hot concentrated sodium hydroxide. The relation between the iron content of the alloy and the concentration of $FeSO_4$ in the deposition electrolyte is shown in Table I. It is definitely clear that the addition of iron to nickel increases the activity for hydrogen evolution, although the mechanism of the hydrogen evolution is not changed by the iron addition, since the Tafel slope, that is about 150 mM/dec, is not changed by alloying. Even if the Fe^{2+} ion content of the solution is less than 1/10 of Ni^{2+} ion the iron content in the deposits becomes about 50 atom %. Figure 2 shows the XRD patterns of the electrodeposited Ni-Fe alloys. Unless the iron content of the deposits exceeds 60 atom %, the body-centered cubic (bcc) phase was not formed,[14] and the alloys shown in Fig. 2 are composed of the single face-centered cubic (fcc) structure, although the lattice constant increases almost linearly with the iron content from 0.3512 nm for Ni to 0.3570 nm for Ni-52.9 atom % Fe alloy. The apparent grain size decreases from 16 nm for nickel to 11 nm for Ni-12.2 atom % Fe and then almost linearly decreases to about 5 nm for Ni-52.9 atom % Fe.

The addition of a complexing agent, lysine, into the nickel deposition solution also remarkably increases the hydrogen evolution activity as shown in Fig. 3. The relation between the carbon content of the alloy and the concentration of lysine in the deposition electrolyte is shown in Table II. The electrodeposits contain carbon together with nickel. Figure 4 shows XRD patterns of the alloys electrodeposited from solutions with Ni^{2+} and lysine. The carbon addition leads to no appreciable change in the lattice constant from that of nickel but to decrease in the average grain size to about 6 nm for Ni-4.3 atom % C alloy. Figure 5 shows an example of the C 1s

* Electrochemical Society Active Member.
** Electrochemical Society Fellow.
[d] Present address: Department of Materials Science and Engineering, Graduate School of Engineering, Hokkaido University, Sapporo 060-8628, Japan.
[z] E-mail: koji@imr.tohoku.ac.jp

S0013-4651(00)01-083-1 CCC: $7.00

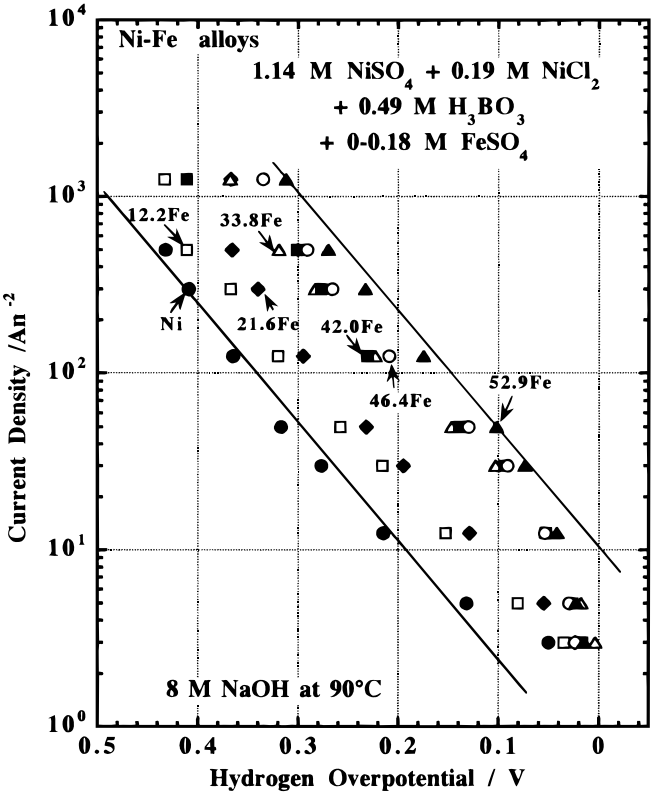

Figure 1. Change in cathodic polarization curves of electrodeposited Ni-Fe alloys for hydrogen evolution in 8 M NaOH at 90°C with alloy composition.

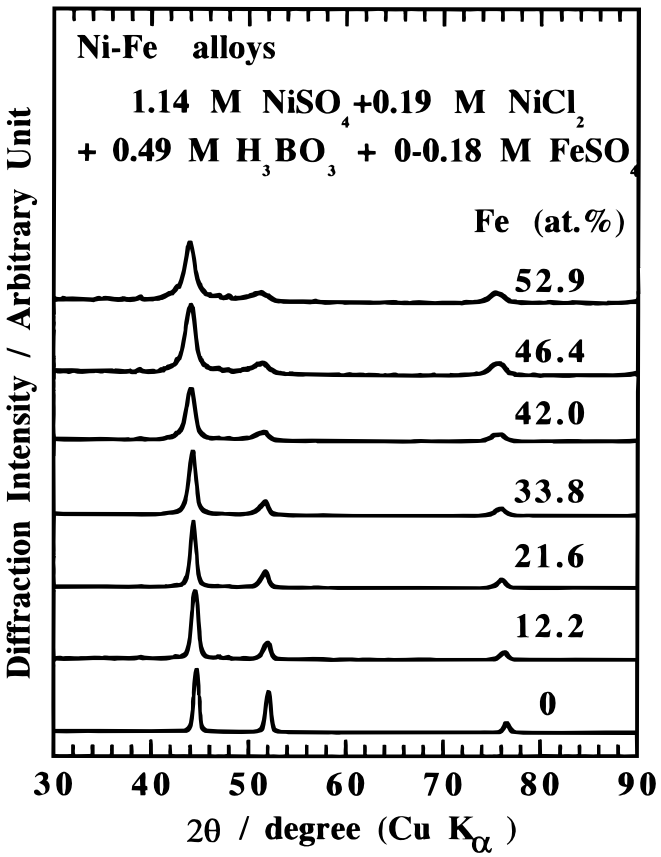

Figure 2. XRD patterns of Ni-Fe electrodeposits with different iron contents. The iron contents of the deposits are written in the figure.

spectrum of the alloy electrodeposited in the solution containing both Ni^{2+} and lysine. The spectrum consists of carbide or graphite-like carbon in addition to the contaminant carbon on the specimen surface. It can, therefore, be said that the fcc solid solution supersaturated with carbon is formed by coelectrodeposition of nickel and carbon. As shown in Fig. 3 the increasing carbon content of the electrodeposits increases the activity for hydrogen evolution as high as inducing the change of the mechanism of the hydrogen evolution, as can be seen from the change in the Tafel slope.

The addition of carbon into iron deposits is further effective in enhancing the activity for hydrogen evolution as shown in Fig. 6. The relation between the carbon content of the alloy and the concentration of lysine in the deposition electrolyte is shown in Table III. As can be seen from a comparison of Fig. 3 and 6, iron is naturally more active than nickel for the hydrogen evolution, and the addition of carbon to iron significiantly increases the activity for hydrogen evolution and is more effective than the addition of carbon to nickel. As shown in Fig. 7, no reflections other than bcc iron were observed in the XRD patterns of these deposits. The changes in the lattice constant and grain size are not large from $a = 0.2862$ nm and 23 nm for iron, respectively, to $a = 0.2878$ nm and 8.7 nm for the Fe-4.1 atom % C

Table I. Change in iron content of electrodeposited Ni-Fe alloys with concentration of $FeSO_4$ in solutions consisting of 1.14 M $NiSO_4$, 0.19 M $NiCl_2$, 0.49 M H_3BO_3, and 0.018-0.18 M $FeSO_4$.

$FeSO_4$ (M)	Fe (atom %)
0.018	12.2
0.036	21.6
0.072	33.8
0.108	42.0
0.144	46.4
0.180	52.9

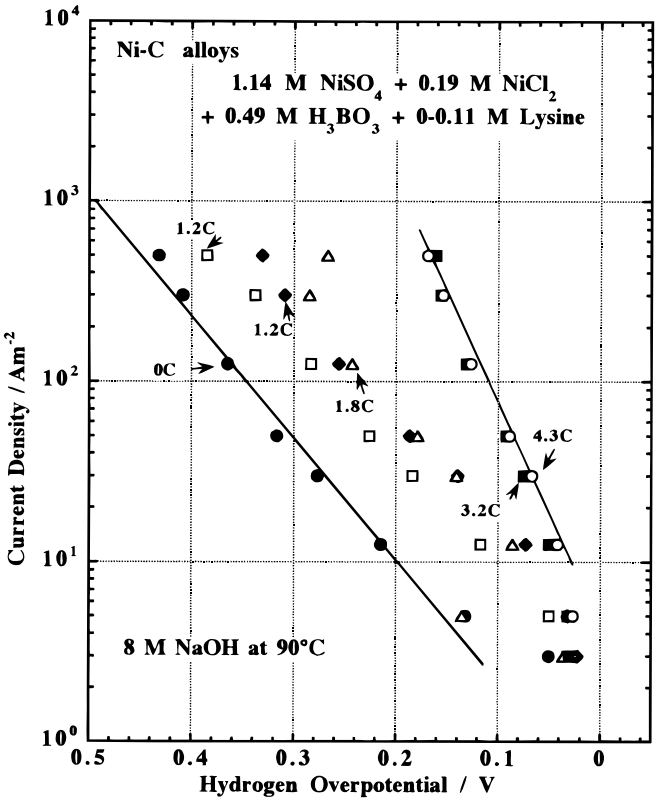

Figure 3. Change in cathodic polarization curves of electrodeposited Ni-C alloys for hydrogen evolution in 8 M NaOH at 90°C with alloy composition.

S0013-4651(00)01-083-1 CCC: $7.00

Table II. Change in carbon content of electrodeposited Ni-C alloys with concentration of lysine in solutions consisting of 1.14 M $NiSO_4$, 0.19 M $NiCl_2$, 0.49 M H_3BO_3, and 0.0011-0.11 M lysine.

Lysine (M)	C (atom %)
0.0011	1.2
0.0055	1.2
0.011	1.8
0.055	3.2
0.11	4.3

alloy, respectively. Accordingly, the formation of bcc iron supersaturated with carbon is remarkably effective in enhancing the activity for hydrogen evolution.

Although the Fe-C cathodes are very active for hydrogen evolution, because the Fe-C cathodes are seriously corroded in hot concentrated sodium hydroxide solutions particularly during open-circuit immersion in the shutdown period of the electrolysis, more durable Ni-Fe-C alloys were prepared by electrodeposition. Figure 8 shows examples of the change in the activity for hydrogen evolution with the addition of lysine into Ni-Fe alloys. The change in iron and carbon contents of the alloy with concentration of lysine in the deposition electrolyte is shown in Table IV. The lysine addition is remarkably effective in enhancing the activity for hydrogen evolution; the addition of 0.0011 M lysine leads to the 2.1 atom % addition of carbon to Ni-Fe alloy and to one order of magnitude increase in the current density for hydrogen evolution, although the mechanism of hydrogen evolution is not changed. When 0.0055 M or more lysine is added, the hydrogen evolution efficiency is remarkably enhanced, and the mechanism of the hydrogen evolution reaction is changed as

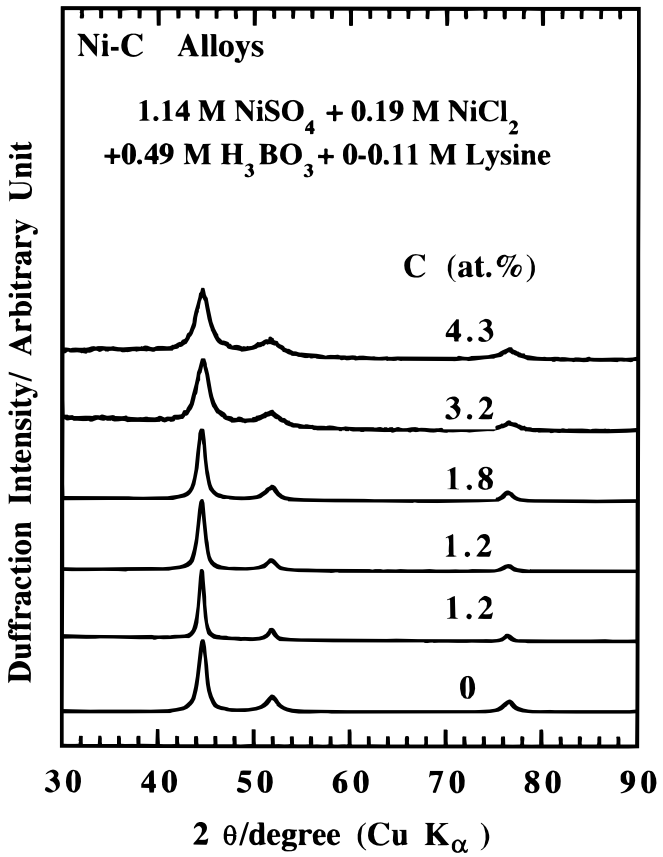

Figure 4. XRD patterns of Ni-C electrodeposits with different carbon contents. The carbon contents of the deposits are written in the figure.

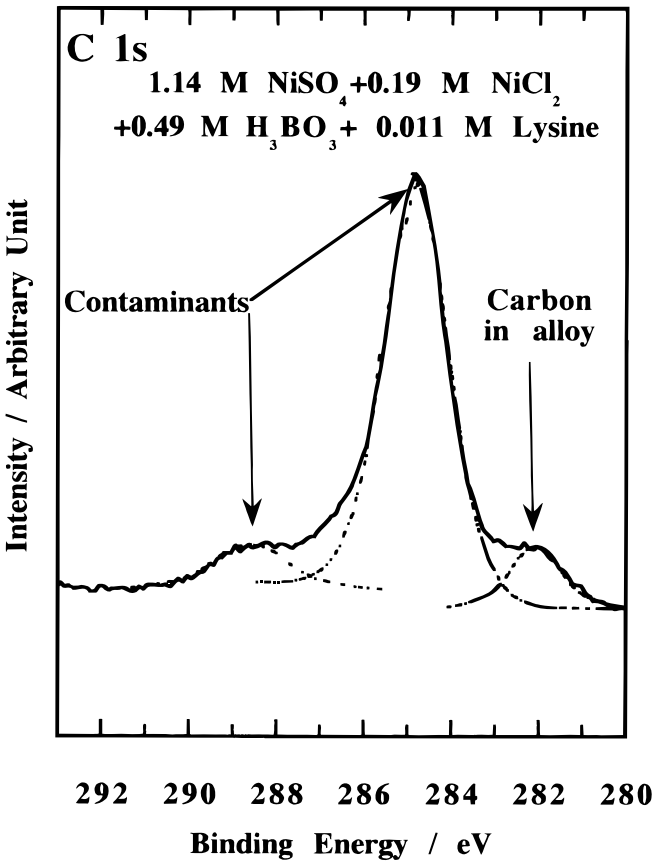

Figure 5. The C 1s spectrum measured from the Ni-1.8 atom % C alloy electrodeposited from a solution consisting of 1.33 M Ni^{2+}, 0.49 M H_3GO_3, and 0.011 M lysine.

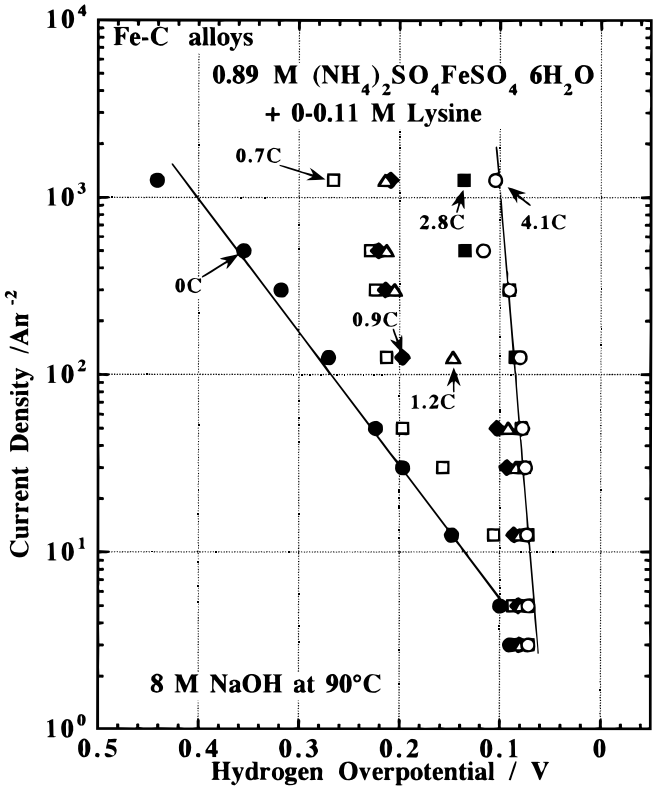

Figure 6. Change in cathodic polarization curves of electrodeposited Fe-C alloys for hydrogen evolution in 8 M NaOH at 90°C with alloy composition.

S0013-4651(00)01-083-1 CCC: $7.00

Table III. Change in carbon content of electrodeposited Fe-C alloys with concentration of lysine in solutions consisting of 0.889 M $(NH_4)_2SO_4FeSO_4$ and 0.0011-0.11 M lysine.

Lysine (M)	C (atom %)
0.0011	0.7
0.0055	0.9
0.011	1.2
0.055	2.8
0.11	4.1

can be seen from the change in the Tafel slope. The Tafel slope of the polarization curves measured from the specimens electrodeposited in the solutions with 0.0055 M or more lysine is about 33 mV/dec. Figure 9 shows XRD patterns of these alloys. When carbon contents are 2.1-4.6 atom %, the extra reflection assumed to be the Fe_2C phase appears at about $2\theta = 42.8°$, in addition to the enhancement of the 110 preferred orientation of the fcc phase. However, the Ni-Fe-C alloys with 5.0 and 7.3 atom % carbon consist of nanocrystalline single fcc phase.

Figure 10 shows the C 1s spectra measured from the Fe-Ni-C alloys electrodeposited from the solution with different lysine contents. When sufficient amounts of lysine are contained in the electrodeposition solutions the C 1s spectra of the alloys show clearly the presence of carbide- or graphite-like carbon which is contained in the nanocrystalline single fcc phase alloys.

Although the Ni-Fe-C alloys electrodeposited from the solutions containing 0.0055 M or more lysine show almost the same very high activity for hydrogen evolution as shown in Fig. 8, since the two

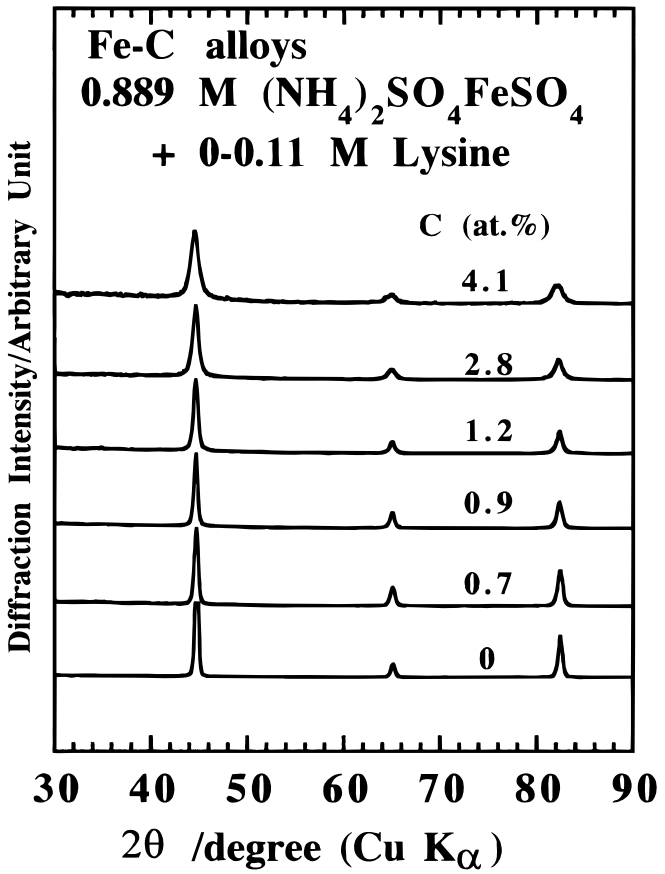

Figure 7. XRD patterns of Fe-C alloys electrodeposited from Fe^{2+}-lysine solutions with different lysine contents. The carbon contents of the deposits are written in the figure.

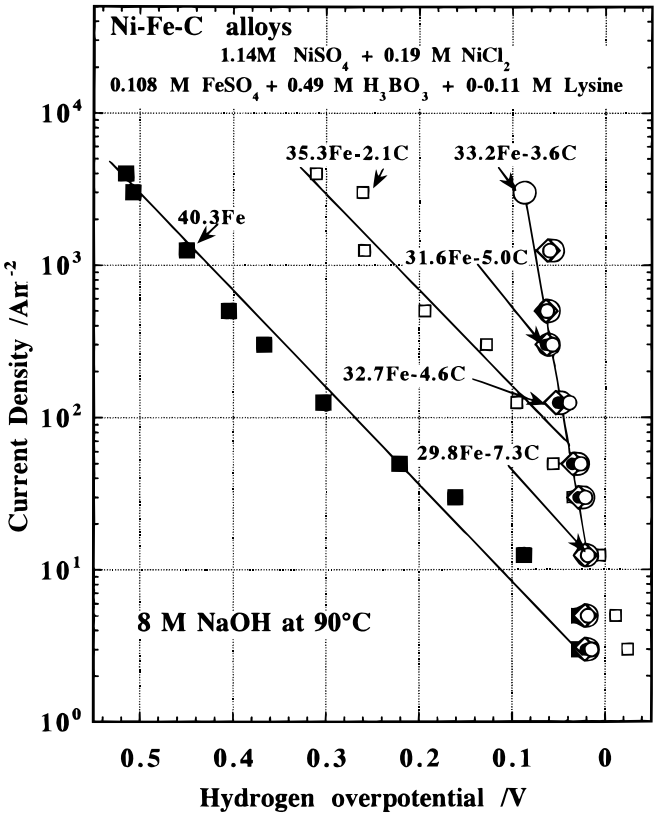

Figure 8. Change in polarization curves of electrodeposited Ni-Fe-C alloys for hydrogen evolution in 8 M NaOH at 90°C with alloy composition.

phase mixtures seem to be unstable during electrolysis and electrolysis shutdown, the addition of 0.055 M or more lysine to the Ni^{2+}-Fe^{2+} solutions for cathodic deposition is preferable. Accordingly, electrodeposition was carried out using the electrolytes containing 0.055 M lysine and different concentrations of Fe^{2+} ions. The polarization curves of these alloys for hydrogen evolution are shown in Fig. 11. The change in iron and carbon contents of the alloy with concentration of $FeSO_4$ in the deposition electrolyte is shown in Table V. The addition of iron to Ni-C alloys is significantly effective in enhancing the activity for hydrogen evolution. The Tafel slope of the alloys with sufficient iron contents is about 33 mV/dec. Figure 12 shows the XRD patterns of these alloys. The alloys with particularly higher iron contents, such as 34.6 atom % or more are nanocrystalline single phase and they show almost the same highest activity for hydrogen evolution.

Figure 13 summarizes the change in cathodic polarization curves with alloying additions. Alloys containing iron and/or carbon were deposited in solutions with fixed concentrations of $FeSO_4$ and/or lysine, respectively. The addition of lysine into the electrolyte for the formation of Fe-C alloy is definitely more effective than the same

Table IV. Change in contents of iron and carbon of electrodeposited Ni-Fe-C alloys with concentration of lysine in solutions consisting of 1.14 M $NiSO_4$, 0.19 M $NiCl_2$, 0.49 M H_3BO_3, 0.108 M $FeSO_4$, and 0-0.11 M lysine.

Lysine (M)	Fe (atom %)	C (atom %)
0	40.3	0
0.0011	35.3	2.1
0.0055	33.2	3.6
0.011	32.7	4.6
0.055	31.6	5.0
0.11	29.8	7.3

S0013-4651(00)01-083-1 CCC: $7.00

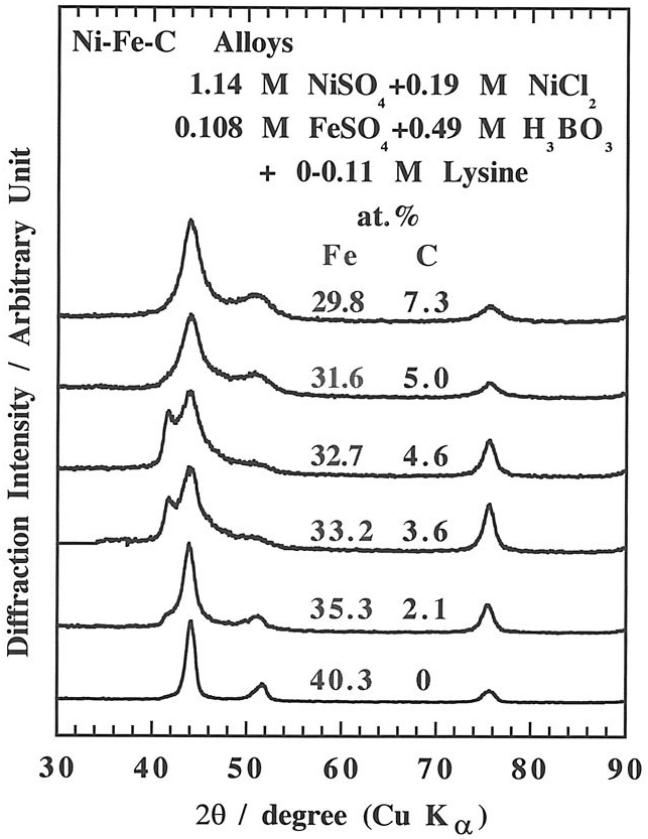

Figure 9. XRD patterns of Ni-Fe-C alloys electrodeposited form Ni^{2+}-lysine-0.108 M $FeSO_4$ solutions with different lysine contents. The analytical results of iron and carbon contents are shown in the figure.

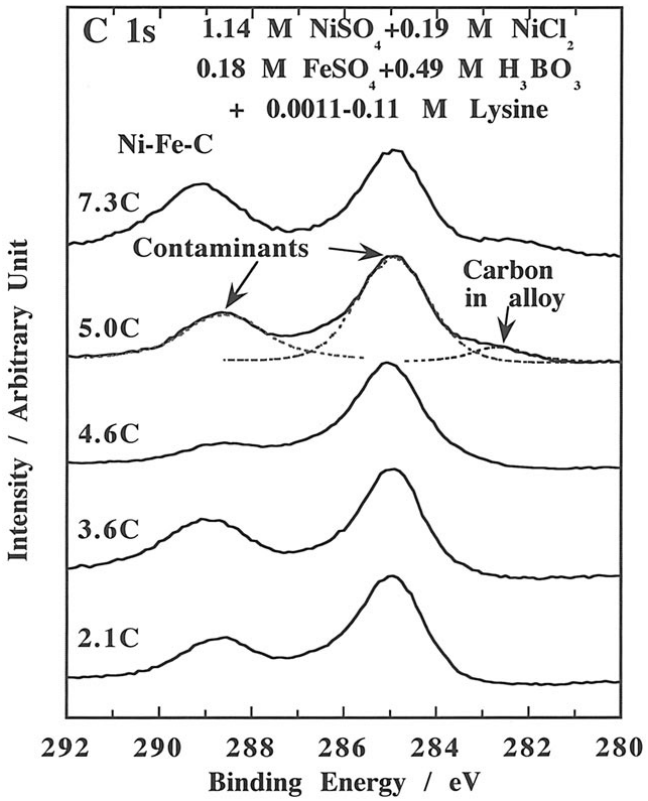

Figure 10. The C 1s photoelectron spectra measured from Ni-Fe-C alloys electrodeposited in Ni^{2+}-lysine-0.18 M $FeSO_4$ solutions with different lysine contents.

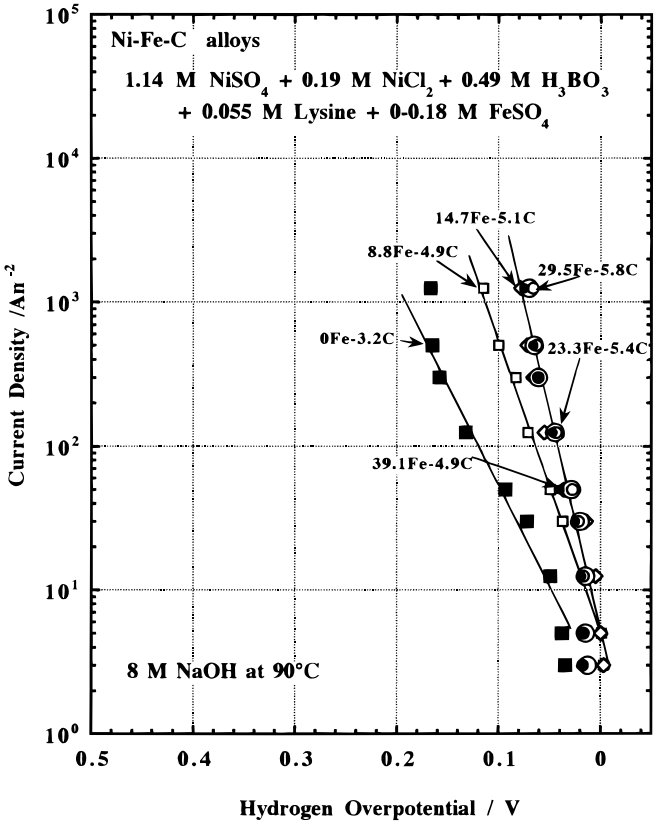

Figure 11. Change in cathodic polarization curves of electrodeposited Ni-Fe-C alloys for hydrogen evolution in 8 M NaOH at 90°C with alloy composition.

amount of lysine addition for the formation of Ni-C alloy. The addition of the same amount of lysine for the formation of Ni-Fe-C alloys is particularly effective in enhancing the hydrogen evolution.

In order to examine the alloying effect on the electronic state of electrode metals, binding energies of core electrons of nickel and iron were examined by XPS. The results are shown in Fig. 14. In binary Ni-Fe alloys the binding energy of the Ni $2p_{3/2}$ electrons increases with increasing the iron content of the alloy, while the binding energy of the Fe $2p_{3/2}$ electrons decreases with increasing the nickel content of the alloy. This is well-known alloying effect and reveals the charge transfer from nickel to iron. When the ternary alloys are formed by containing carbon the charge transfer from the nickel to iron is further singificantly enhanced.

Discussion

In order to tailor cathodes with the high activity for hydrogen evolution in chlor-alkali electrolysis and/or seawater electrolysis, alloying of nickel with iron and carbon was attempted. When the cathodic polarization curves of nickel (Fig. 1 and 3) and iron (Fig. 6)

Table V. Change in contents of iron and carbon of electrodeposited Ni-Fe-C alloys with concentration of $FeSO_4$ in solutions consisting of 1.14 M $NiSO_4$, 0.19 M $NiCl_2$, 0.49 M H_3BO_3, 0.055 M lysine, and 0.018-18 M $FeSO_4$.

$FeSO_4$ (M)	Fe (atom %)	C (atom %)
0	0	3.2
0.018	8.8	4.9
0.036	14.7	5.1
0.072	23.3	5.4
0.108	29.5	5.8
0.144	34.6	5.4
0.180	39.1	4.9

S0013-4651(00)01-083-1 CCC: $7.00

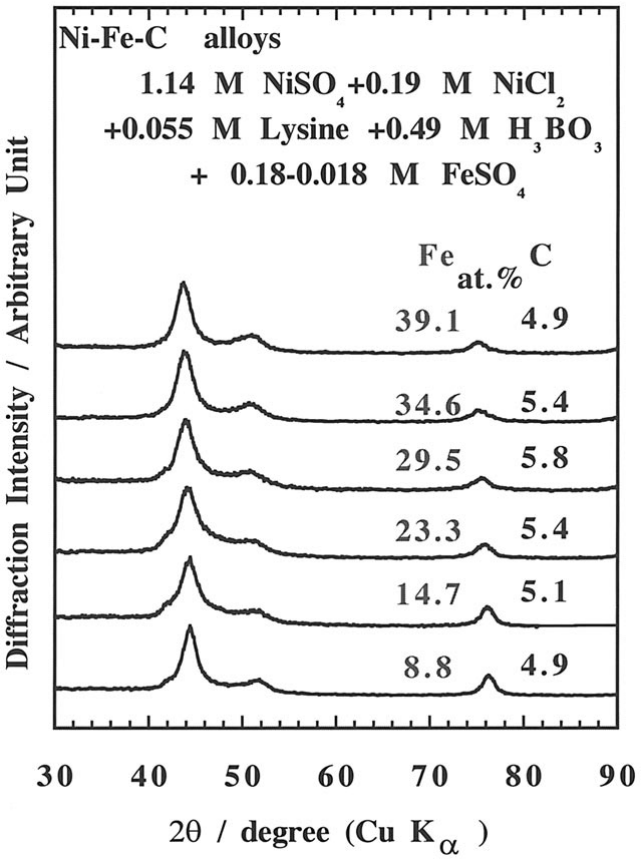

Figure 12. XRD patterns of Ni-Fe-C alloys electrodeposited form Ni^{2+}-Fe^{2+}-0.055 M lysine solutions with different $FeSO_4$ contents. Iron and carbon contents of the alloys are shown in the figure.

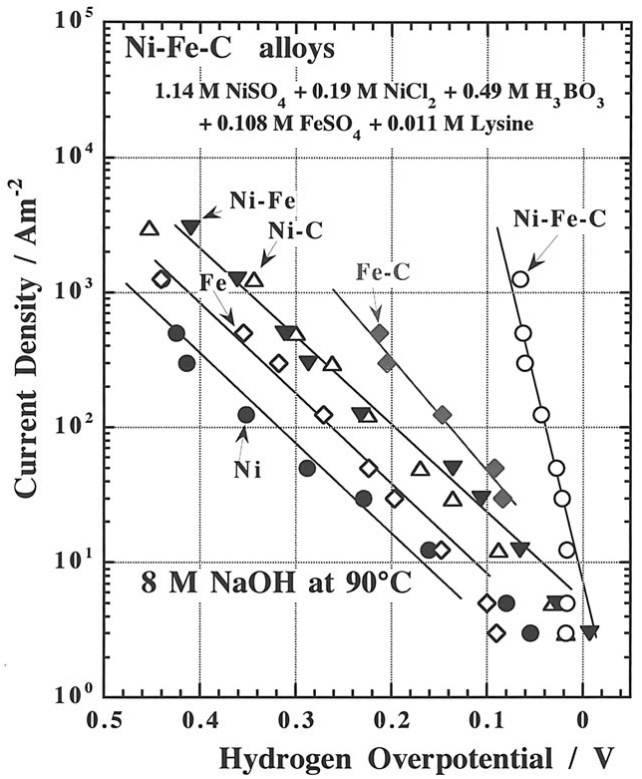

Figure 13. Comparison of cathodic polarization curves of Ni, Fe, Ni-Fe, Ni-C, Fe-C, and Ni-Fe-C electrodeposits for hydrogen evolution in 8 M NaOH at 90°C.

are compared, iron has a higher activity than nickel for hydrogen evolution. As can be seen in Fig. 1 and 6, binary Ni-Fe alloys show higher activities for hydrogen evolution than those of nickel and iron metals. The Tafel slope of nickel, iron, and Ni-F alloys is almost the same as each other, and about 150 mV/dec, that is, $\partial E/\partial(\log i) = 2RT/F$. If we assume the surface coverage of adsorbed hydrogen is close to zero and the transfer coefficient is 0.5, the proton discharge seems to be the rate-determining step (rds) for hydrogen evolution.[15,16] Accordingly, if nickel and iron atoms are present on the electrode surface, the proton discharge occurs preferentially on more active iron atoms. As can be seen in Fig. 14 the charge transfer occurs from nickel to iron. This act suggests that the rate-determining proton discharge receiving electrons from surface iron atoms is accelerated by the charge transfer from nickel to iron. Therefore, the higher activity of Ni-Fe alloys than nickel and iron metals for hydrogen evolution is attributable to the acceleration of the proton discharge as a result of charge transfer from nickel to iron by alloying.

When carbon is added to Ni-Fe alloys the hydrogen evolution is remarkably accelerated, changing the mechanism of the hydrogen evolution. The Tafel slope becomes about 33 mV/dec. If we assume that the surface coverage of adsorbed hydrogen is close to zero and that the transfer coefficient is 0.5, when the desorption of adsorbed hydrogen by recombination is the rds, $\partial E/\partial(\log i = RT/2F$, that is, 36 mV/dec. This suggests that the carbon addition significantly accelerates the proton discharge on iron so that the rds is no longer proton discharge but is desorption of adsorbed hydrogen. Figure 14 shows that the addition of carbon into Ni-Fe alloys considerably enhances

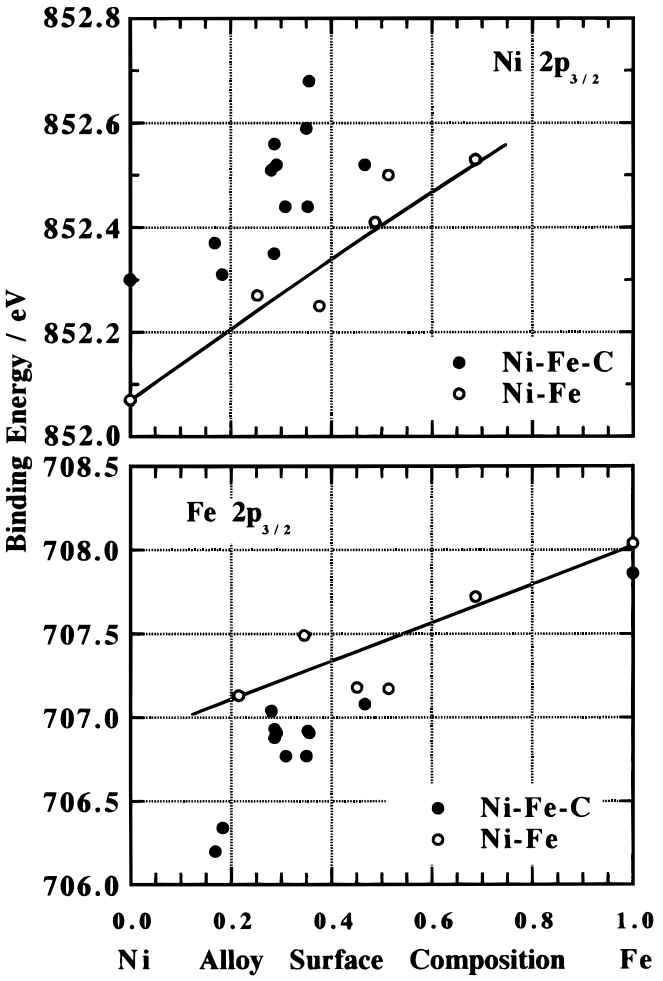

Figure 14. The binding energies of Ni $2p_{3/2}$ and Fe $2p_{3/2}$ electrons in electrodeposited Ni-Fe-C and Ni-Fe alloys as a function of mole fraction of iron (Fe/Ni + Fe) in the deposits.

S0013-4651(00)01-083-1 CCC: $7.00

the charge transfer from nickel to iron. Accordingly, the charge transfer from iron to proton for the proton discharge seems much easier by alloying with carbon.

In conclusion, the formation of ternary Ni-Fe-C alloys leads to a significant charge transfer from nickel to iron, to accelerated electron transfer from iron to proton, and to accelerated proton discharge, with a consequent remarkable acceleration of the hydrogen evolution.

These cathodes maintain the high activity for hydrogen evolution in chlor-alkali electrolysis for more than 2 years and the high activity is not degraded by shutdown of electrolysis.[17] Furthermore, after construction of industrial electrolysis cells using expanded-nickel cathodes for chlor-alkali electrolysis, the Ni-Fe-C alloy cathodes have been successfully prepared by electrodeposition on the nickel cathodes.

Conclusions

Electrodeposition was employed to tailor active and durable nickel alloy cathodes for hydrogen evolution in 8 M naOH at 90°C. The following conclusions can be drawn

1. The activity of iron for hydrogen evolution is naturally higher than that of nickel.

2. Formation of Ni-Fe alloys results in significant enhancement of hydrogen evolution and the activity of the Ni-Fe alloys for hydrogen evolution is higher than iron and nickel metals, although the Tafel slope for cathodic reaction, that is, about 150 mV/dec, is unchanged, suggesting no change in the mechanism of hydrogen evolution.

3. When carbon is added to iron or nickel by adding complexing agent, lysine, into electrodeposition solutions, the electrodeposits contain carbide- or graphite-like carbon and the remarkable enhancement of hydrogen evolution takes place so as to change the mechanism of hydrogen evolution. The activity of Fe-C electrodes is higher than that of Ni-C electrode.

4. Electrodeposited Ni-Fe-C alloys are most active for hydrogen evolution, and the Tafel slope becomes about 33 mV/dec.

5. XPS analysis reveals that charge transfer occurs from nickel to iron in binary Ni-Fe alloys and charge transfer is further enhanced by the formation of ternary Ni-Fe-C alloys.

6. The enhanced charge transfer to iron in the ternary alloy seems responsible for acceleration of proton discharge so as to change the rate-determining step (rds) from proton discharge to desorption of adsorbed hydrogen.

Acknowledgment

The authors express their acknowledgment to Analytical Research Core for Advanced Materials, Institute for Materials Research, Tohoku University, for carbon analysis.

Tohoku Institute of Technology assisted in meeting the publication costs of this article.

References

1. H. Vanderborre, Ph. Vermeiren, and R. Leysen, *Electrochim. Act*, **29**, 297 (1984).
2. E. Endoh, H. Otouma, T. Morimoto, and Y. Oda, *Int. J. Hydrogen Energy*, **12**, 473 (1987).
3. J.-Y. Huot, *J. Electrochem. Soc*., **136**, 1933 (1989).
4. E. Beltowska-Lehman, *J. Appl. Electrochem*., **20**, 132 (1990).
5. D. E. Brown, M. N. Mehmood, M. C. M. Man, and A. K. Turner, *Electrochim. Acta*, **29**, 1551 (1984).
6. J.-Y. Huot, M. L. Trudeau, and R. Schulz, *J. Electrochem. Soc*., **138**, 1316 (1991).
7. D. Miousse, A. Lasia, and V. Borck, *J. Appl. Electrochem*., **25**, 592 (1995).
8. A. Kawashima, E. Akiyama, H. Habazaki, and K. Hashimoto, *Mater. Sci. Eng*., **A226-228**, 905 (1998).
9. C. Iwakura, N. Furukawa, and M. Tanaka, *Electrochim. Acta*, **37**, 757 (1992).
10. H. Yamashita, T. Yamamura, and K. Toshimoto, *J. Electrochem. Soc*., **140**, 2238 (1993).
11. R. Schulz, J.-Y. Huot, M. L. Trudeau, L. Dignard-Bailey, Z. H. Yan, S. Jin, A. Lamarre, E. Ghali, and A. van Neste, *J. Mater. Res*., **9**, 2998 (1994).
12. A. Kawashima, T. Sakaki, H. Habazaki, and K. Hashimoto, *Mater. Sci. Eng*., **A267**, 246 (1999).
13. P. Scherrer, *Götingen Nachr*., **2**, 98 (1918).
14. W. B. Pearson, *A Handbook of Lattice Spacings and Structures of Metals and Alloys*, p. 639, Pergamon Press, London (1958).
15. S. Trasatti, in *Advances in Electrochemical Science and Engineering*, H. Gerischer and C. W. Tobias, Editors, Vol. 2, p. 1, VCH, Weinheim (1992).
16. A. Kawashima, K. Hashimoto, and S. Shimodaira, *Corrosion*, **32**, 321 (1976).
17. K. Suetsugu, T. Sakaki, K. Yoshimitsu, K. Yamaguchi, A. Kawashima, and K. Hashimoto, *Chlor-Alkali and Chlorate Technology*, H. S. Burney, N. Furuya, F. Hine, and K.-I. Ota, Editors, PV 99-21, p. 169, The Electrochemical Society Proceedings Series, Pennington, NJ (1999).